Computation of complexity measures of morphologically significant zones decomposed from binary fractal sets via multiscale convexity analysis

Sin Liang Lim [a,*], Voon Chet Koo [a], B.S. Daya Sagar [b]

[a] Faculty of Engineering and Technology, Melaka Campus, Multimedia University, Jalan Ayer Keroh Lama, 75450 Melaka, Malaysia
[b] Indian Statistical Institute-Bangalore Centre, 8th Mile, Mysore Road, RV College PO, Bangalore 560059, India

ARTICLE INFO

ABSTRACT

Multiscale convexity analysis of certain fractal binary objects—like 8-segment Koch quadric, Koch triadic, and random Koch quadric and triadic islands—is performed via (i) morphologic openings with respect to recursively changing the size of a template, and (ii) construction of convex hulls through half-plane closings. Based on scale vs convexity measure relationship, transition levels between the morphologic regimes are determined as crossover scales. These crossover scales are taken as the basis to segment binary fractal objects into various morphologically prominent zones. Each segmented zone is characterized through normalized morphologic complexity measures. Despite the fact that there is no notably significant relationship between the zone-wise complexity measures and fractal dimensions computed by conventional box counting method, fractal objects—whether they are generated deterministically or by introducing randomness—possess morphologically significant sub-zones with varied degrees of spatial complexities. Classification of realistic fractal sets and/or fields according to sub-zones possessing varied degrees of spatial complexities provides insight to explore links with the physical processes involved in the formation of fractal-like phenomena.

1. Introduction

Fractal sets and functions are replica of various natural features such as lakes, porous medium, threshold sets representing spatial patterns of rainfall, temperature (sets), and spatial fields such as rainfall, temperature, clouds, vegetation, elevations, and landscapes (functions). Spatial objects (e.g. binary fractal shapes) and fields (e.g. fractal functions) with varied degrees of spatial complexities possess various morphologically significant regions within. Characterization of complete spatial objects and/or functions via fractal methods (e.g. box dimension) has been attempted by several researchers (e.g. [1,2]). One of the elegant ways of computing fractal dimension of spatially represented fractal sets and/or functions is conventional box counting method [1], and cube counting method (e.g. [3–5]). Generalized dimension computation (e.g. [6]) has also been proven to be powerful. Those methods that employed mathematical morphologic transformations to compute the fractal dimension of spatial objects and functions include boundary dilation method [7] and Minkowski–Bouligand dimension [8]. By converting spatial set into an abstract structure like skeletal network, a relationship between the ratio of number of skeletal segments of successive orders and the ratio of mean lengths of skeletal segments of successive orders is demonstrated on a fractal Koch Quadric shape [9]. Of late, morphologic transformations are employed to decompose a fractal set into non-overlapping disks, and a number-radius relationship—that imitates conventional dimension computation

---

* Corresponding author.
 E-mail address: lim.sin.liang@mmu.edu.my (S.L. Lim).

methods—is provided [10–13]. In another study, a function representing digital elevations is generated at multiscales by employing non-linear multiscale morphologic transformation, and the unique topologic networks such as channel and ridge networks are extracted from multiscale functions [14,15]. Further, a relationship between the scale parameter and network length is shown as a fractal power-law exponent. Besides, an alternative approach to segment and characterize cloud fields retrieved from MODIS (Moderate Resolution Imaging Spectroradiometer) into morphologically significant regions *via* multiscale convexity analysis is investigated in [19]. Application of mathematical morphology is also shown to derive a host of scaling relationships for a large number of water bodies of various sizes and shapes distributed over a geographic space [16].

Characterization of morphologically significant regions that could be decomposed from a spatial object and/or a spatial field has not hitherto been investigated. We investigate a binary Koch Quadric fractal via multiscale convexity analysis with an aim to segment it into morphologically significant regions, and further to characterize each segmented region by deriving region-wise morphologic entropy. This investigation is categorized into six steps: (i) generation of multiscale fractals, (ii) construction of convex hulls of multiscale fractals, (iii) estimation of convexity measures of multiscale fractals, (iv) derivation of morphologically significant threshold scales through graphical relationship plotted between scale parameter and convexity measures, (v) partition of fractal into morphologically significant regions based on threshold scales, and (vi) derivation of roughness indices for each segmented zone. Mathematical morphologic transformations such as multiscale
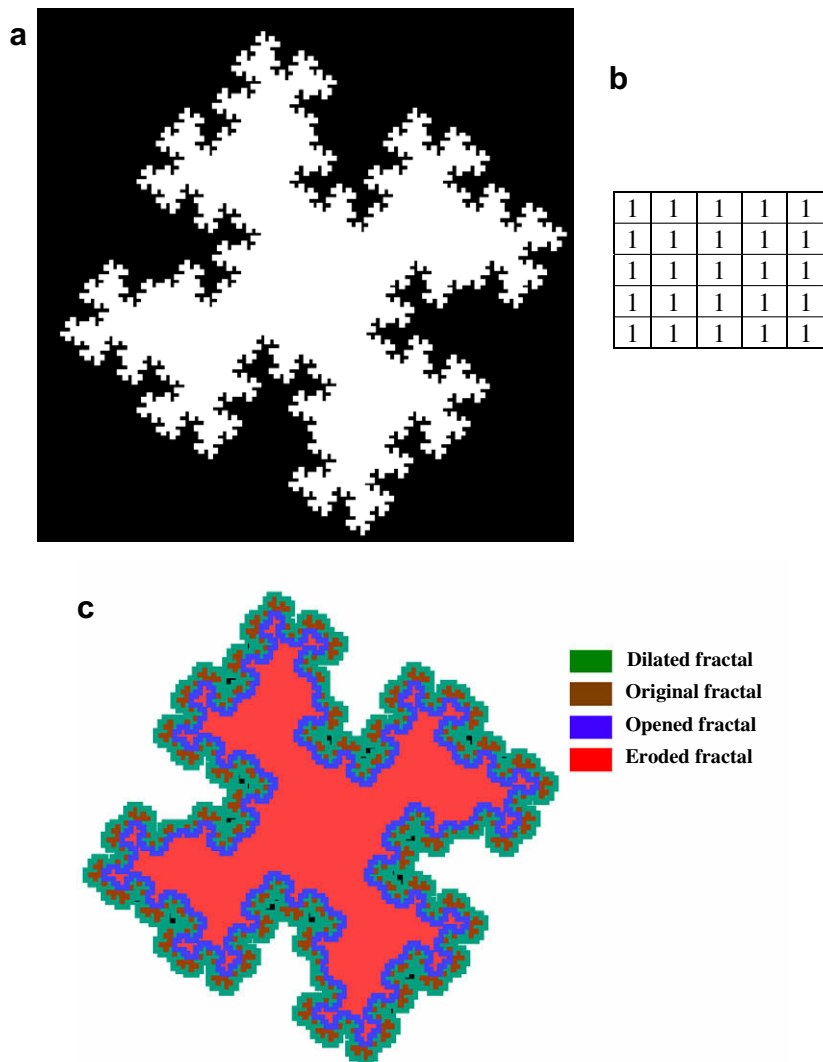

Fig. 1. (a) Binary Koch quadric fractal, (b) structuring element – square, with size 5 × 5, and (c) dilated, original, opened, and eroded fractal coded by green, brown, blue, and red colours respectively. (For interpretation of the references to colour in this figure legend, the reader is referred to the web version of this article.)

opening, half-plane closing, certain logical operations like union, intersection, difference, point-wise minimum, and color coding techniques are employed to deal with this six-step investigation. A binary Koch Quadric fractal of size 400×400 pixels is chosen to implement this six-step approach to meet the aim of the paper. This fractal is partitioned into morphologically significant zones with respect to probing rule, square of primitive size of 5×5. Further, roughness indices are estimated for each segmented zone of a fractal. This investigation offers new insights to quantitative characterization of spatial objects, trees, and fields.

## 2. Fractal set and basic mathematical morphologic transformations

Let M be a fractal set (e.g. Fig. 1a)—generated up to second iteration by choosing a square set as initiator and a generating rule ([17], p. 350)—of size 400×400 pixels. The translation invariant set operations δ_B and $\in_B$ defined by $\delta_B(M) = M \oplus B$ and $\in_B = M \ominus B, \forall M \in R^2$ are the dilation (Fig. A1a) and erosion (Fig. A1b) by a symmetric flat structuring element B. As B (Figs. 1b, and A1) is flat and symmetric about origin, these set operations—similar to Minkowski addition and Minkowski subtraction—are written as $M \oplus B = \bigcup_{b \in B} M_b$ and $M \ominus B = \bigcap_{b \in B} M_b$, respectively. An opening transformation (e.g. Fig. A1c), being a morphologic transformation, is defined as erosion followed by dilation, i.e., $M \circ B = (M \ominus B) \oplus B$. By performing dilations and erosions recursively, one can obtain multiscale dilations and erosions that can be written, by imposing the size parameter n of B, in the form of $M \oplus nB$, $M \ominus nB$ respectively, where $n = 0,1,2, \cdots, N$. Further, multiscale opening can be formed as $M \circ nB = (M \ominus nB) \oplus nB$, $n = 0,1,2, \cdots, N$, with $(M \circ NB) \neq \phi$ such that $(M \circ (N + 1)B) = \phi$.

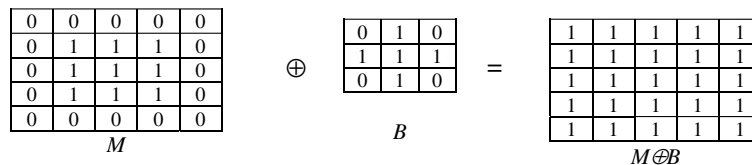## 3. Multiscale fractals and convex hulls, convexity measures

3.1. Generation of multiscale fractals and convex hulls

We generated multiscale binary fractal by employing multiscale opening transformation by means of a square structuring element (B) (Fig. 1b) of primitive size 5×5. The Nth value for B is determined as 21 as $(M \circ 21B) \neq \phi$ such that $(M \circ 22B) = \phi$ as N and $N + 1$, respectively denote 21 and 22. For better visualization, multiscale fractals are colour-coded and superposed (Fig. 2a). The corresponding convex hulls (the construction of which is done by following Soille's [18] algorithm is explained in Appendix A.2) of multiscale fractals are constructed by considering their exterior points. These convex hulls are also colour-coded and superposed (Fig. 2b).

(a) Morphological erosion of M by B
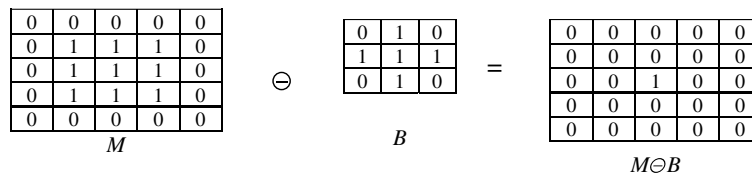
(b) Morphological dilation of M by B

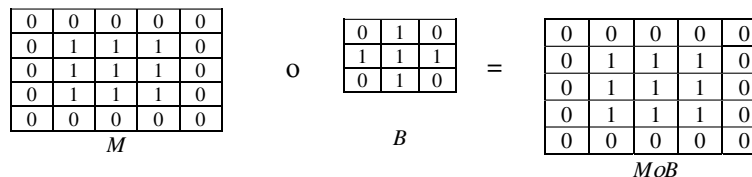(c) Morphological opening of M by B

Fig. A1. Binary morphological transformations. (a) Erosion, (b) dilation, and (c) opening.

3.2. Areas of multiscale fractals and convex hulls

Area of multiscale opening versions of a binary fractal set M by choosing the flat and symmetric structuring element of size n is denoted by $A(M \circ nB)$ where $n = 0, 1, 2, \ldots, N$. The higher the nth value, the larger is the size of B. Let $(M \circ nB)$ be a fractal set opened by nth size of B. Then $(M \circ (n + 1)B) \subseteq (M \circ nB)$ implies that the opened fractal by $(n + 1)$th size B, $(M \circ (n + 1)B)$ is an improper subset of fractal opened by nth size of B, $(M \circ nB)$. Let the area of opened set be $A(M \circ nB)$. Then $A(M \circ nB) \geqslant A(M \circ (n + 1)B)$. Convex hull of the opened set $(M \circ nB)$ is defined as the smallest convex set that contains $(M \circ nB)$, and is denoted by $CH(M \circ nB)$. An opened set $(M \circ nB)$ and its convex hull $CH(M \circ nB)$ are the same if and only if both the sets are exactly identical. Let $CH(M \circ nB)$ and $CH(M \circ (n + 1)B)$ respectively be convex hulls of sets opened by increasing sizes of B. Then $CH(M \circ (n + 1)B) \subseteq CH(M \circ nB)$ further implies that $A[CH(M \circ (n + 1)B)] \leqslant A[CH(M \circ nB)]$.

3.3. Convexity measure

The rate at which the area changes from $(M \circ nB)$ to $(M \circ (n + 1)B)$ is higher than that of the corresponding convex hulls $CH(M \circ nB)$ to $CH(M \circ (n + 1)B)$ (Fig. 2c). The convexity measure of the nth degree opened set is defined as the ratio of the areas of nth degree opened set and its convex hull as $CM(M \circ nB) = \frac{A(M \circ nB)}{A[CH(M \circ nB)]}$, which would be in the range of 0 and 1. An opened set with $CM(M \circ nB)$ of 1 attributes the fact that the opened set itself is highly convex, and $CM(M \circ nB)$ is 0 if and only if $(M \circ nB)$ is a well connected set with maximum possible perforations. Convexity measures $CM(M)$ of multiscale fractals, generated through multiscale morphologic transformation, are estimated by taking the ratio of areas of fractal $A[M \circ nB]$ and its convex hull $A[CH(M \circ nB)]$ at specific scale (n).
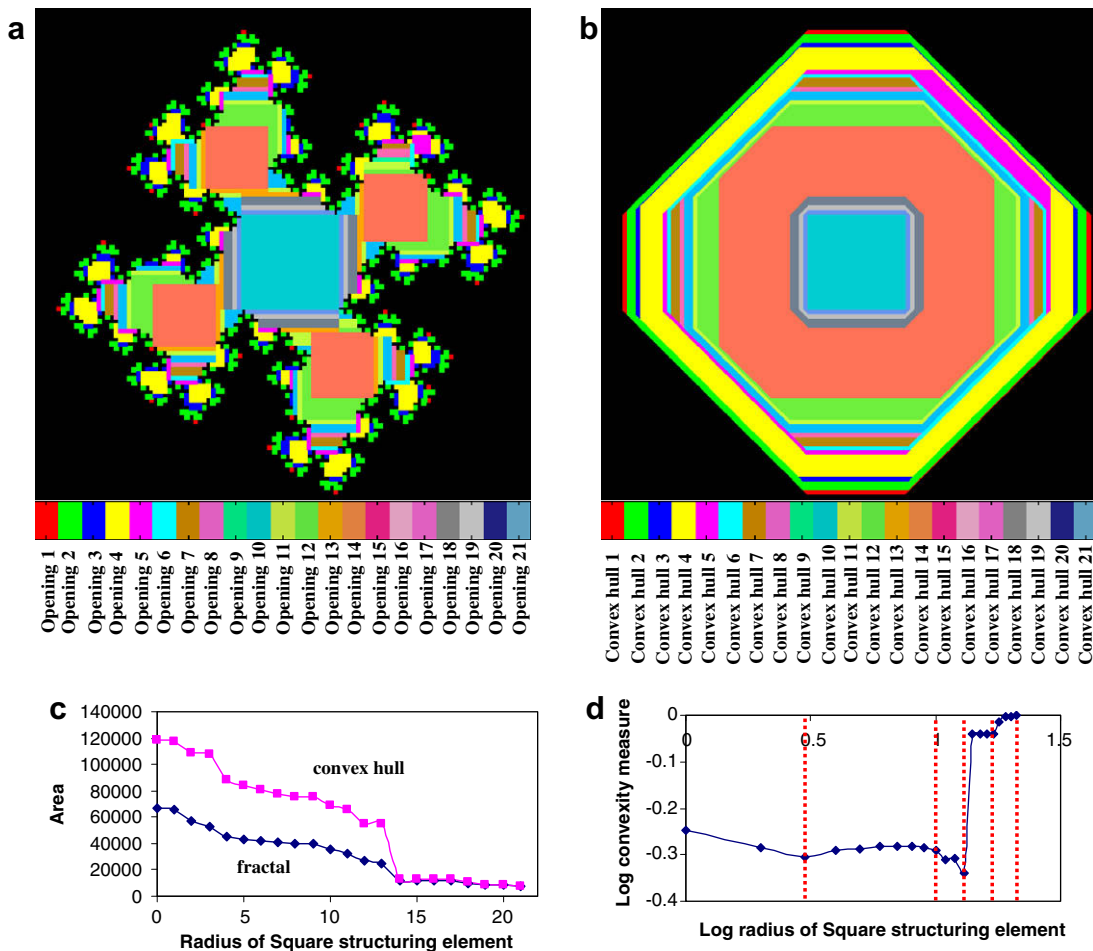

Fig. 2. (a) Opened fractal at multiscales, (b) convex hull of opened fractal at multiscales, (c) area of fractal and its convex hull, at increasing size of square structuring element, and (d) convexity measure at increasing size of square structuring element in logarithmic representation.

4. Partition (segmentation) of binary fractal into topologically prominent regions

The rate of change in convexity measure of an evolving binary fractal (M)—under the influence of recursive scale-based opening transformation—is taken as the basis to partition M into topologically prominent regions. The convexity measures at all scales are plotted as function of scale parameter (n) employed to generate multiscale fractals (Fig. 2d). This graphical relationship is taken as the basis to determine the transition zones between the morphologic phases. These determined transition levels are nothing but the threshold level of opening cycle number at which the morphologic constitution of fractal shape shows significant change. For the two iteration Koch Quadric fractal considered, these threshold opening levels are determined as opening cycles of 0, 3, 10, 13, 17, and 21. Fractal after zeroth-cycle opening retains as original M since zeroth size of structuring element is empty. Fractal at these threshold opening levels are respectively color-coded and superposed (Fig. 3a), and their corresponding convex hulls are also shown in similar fashion (Fig. 3b).

4.1. Isolation of topologically prominent zones

The topologically prominent zones (M_i) are isolated by systematically employing the fractal structures at threshold opening levels. For the fractal under investigation, zone 1 (M_1) is isolated by subtracting the first threshold opening level of fractal (i.e., $M \circ 3B$) from the original fractal (i.e., $M \circ 0B$). Second zone is isolated by subtracting ($M \circ 10B$)—being the second threshold opening level determined from graphical relationship shown in Fig. 4b—from ($M \circ 3B$). In similar fashion other zones are also isolated. The union of six isolated zones leads to the original fractal. These isolated zones are illustrated in a specific order in Fig. 4a-f.

$$M_i = [M \circ (K_{i-1})B] \setminus [M \circ (K_i)B] \tag{1}$$

$$M = \bigcup_{i=1}^{I} M_i \tag{2}$$

$$A[M] = A\left[\bigcup_{i=1}^{I} M_i\right] \tag{3}$$

This isolation process is shown in Eq. (1) where K_i is threshold opening cycle number to obtain i segmented zone (M_i). $K_1, K_2, \cdots, K_{I-1}, K_I$ are threshold opening cycle numbers derived at morphologic transitions obtained at crossover scales. $i = 0, 1, \cdots, I$; and $K_0 = 0$, $K_1 = 3$, $K_2 = 10$, $K_3 = 13$, $K_4 = 17$, $K_{5=I} = 21$, and $K_I + 1 = 22$.
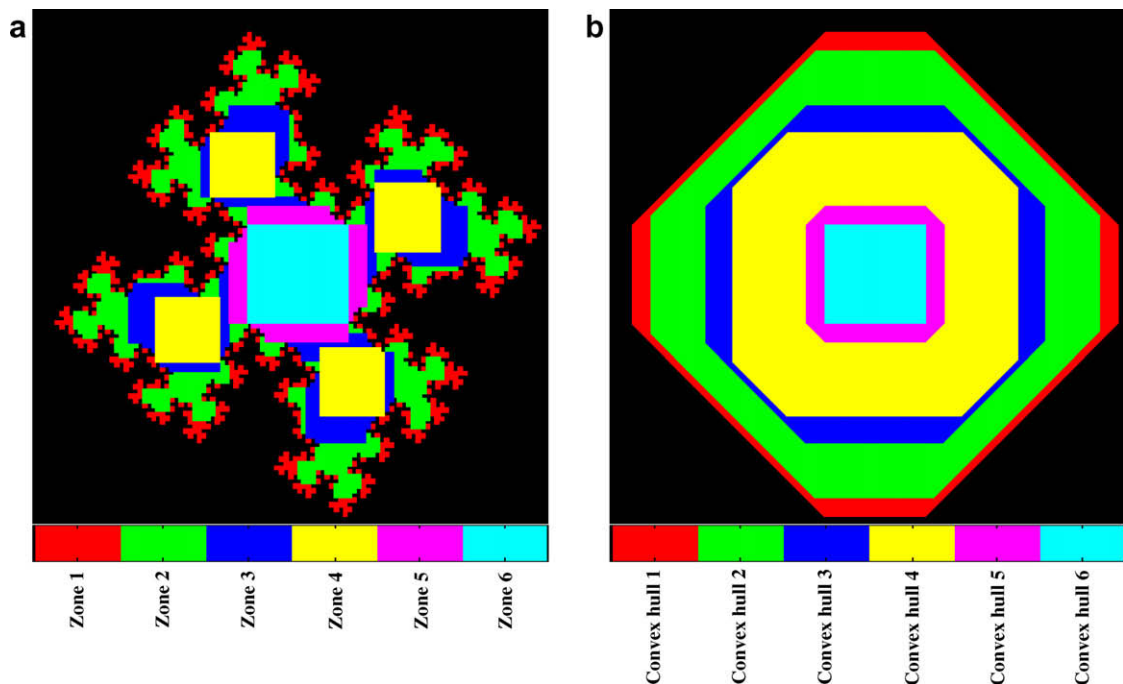

Fig. 3. (a) Opened fractal at crossover scales, and (b) convex hulls of crossover scale opened fractals.
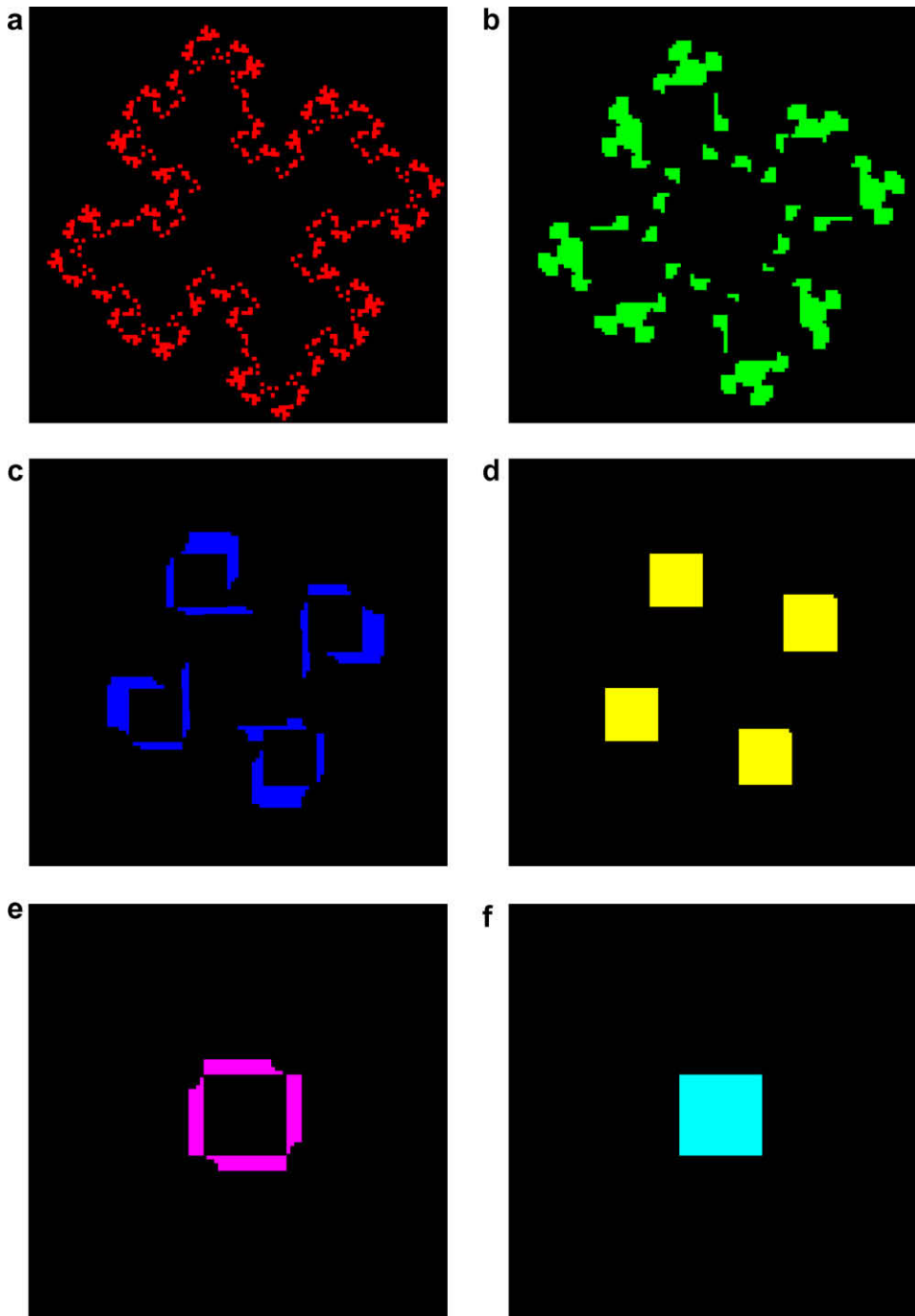
Fig. 4. Zones segmented from Quadric fractal object. (a) M_1, (b) M_2, (c) M_3, (d) M_4, (e) M_5, and (f) M_6.

5. Morphologic complexity of zones decomposed from binary fractal

Probability distribution values at nth-cycle for ith segmented zone is computed according to Eq. (4):

$$p_n(M_i) = \frac{A\{[(M \circ nB) \setminus (M \circ (n+1)B)] \cap [M_i]\}}{A[M_i]} \qquad (4)$$

where $n = 0,1,2,\cdots,N$; $i = 1,2,\cdots,I$. Numerator in this equation represents area of the portion obtained through intersection of ith segmented zone isolated from fractal (M) and portion obtained by subtracting $(n+1)$th opened version (i.e.,

Table 1
Complexity measures of morphologically significant zones decomposed from various fractal shapes (islands)

Fractal type	Zone 1		Zone 2		Zone 3		Zone 4		Zone 5		Zone 6		FD
	CM	NCM	CM	NCM	CM	NCM	CM	NCM	CM	NCM	CM	NCM	
Quadric	1.05	0.35	2.21	0.31	1.47	0.49	0	0	1.52	0.38	0	0	1.74
Random quadric	1.92	0.48	1.53	0.51	1.78	0.36	1.10	0.27	0.93	0.47	0	0	1.69
Triadic	1.81	0.36	2.42	0.19	0.81	0.27	2.00	0.29	1.65	0.06	0	0	1.8
Random triadic	2.20	0.44	1.88	0.47	2.34	0.29	2.16	0.27	1.75	0.19	0	0	1.76

[*] CM = complexity measure, NCM = normalized complexity measure, FD = fractal dimension computed via box counting method.
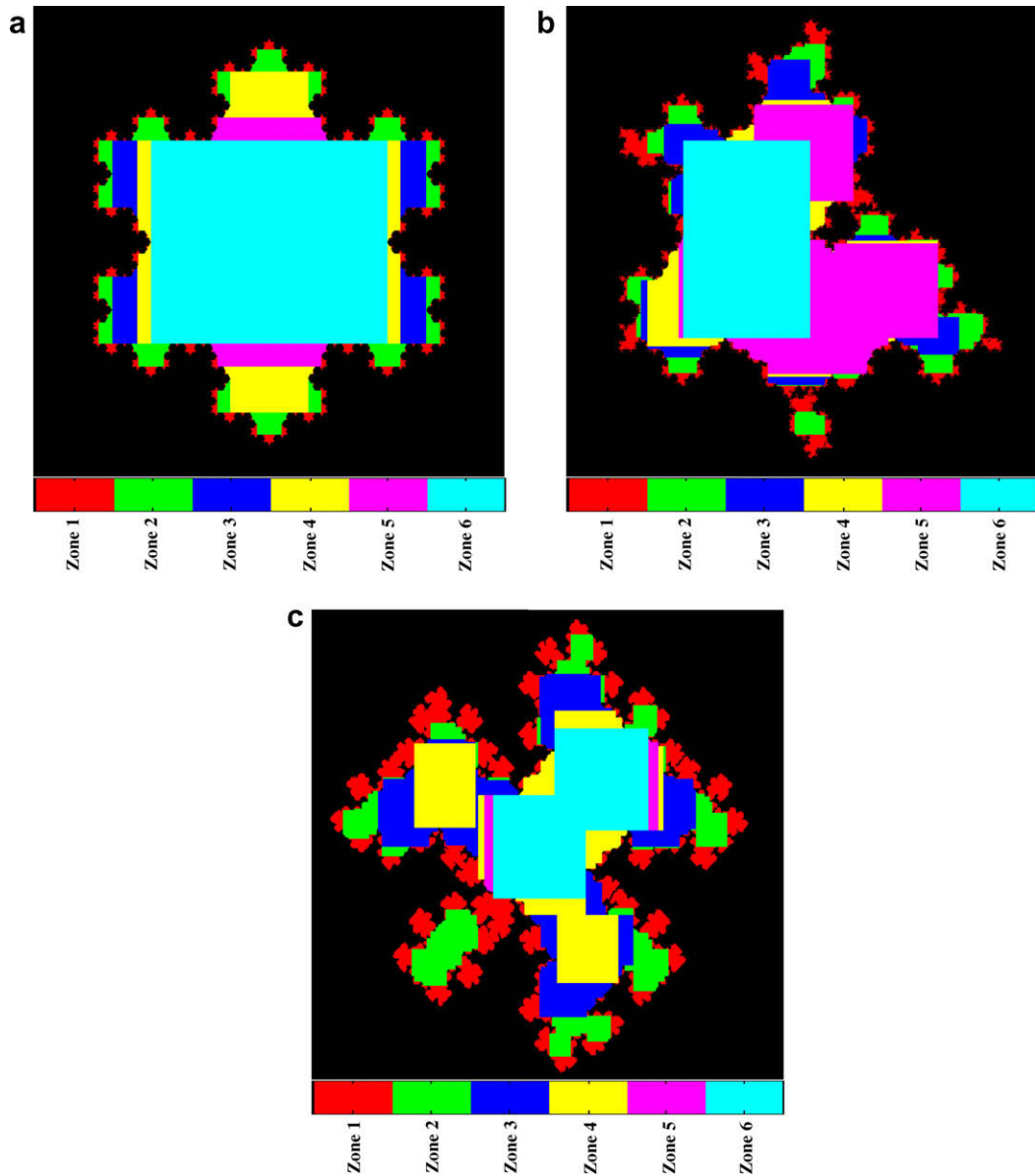
Fig. 5. Morphologically significant zones decomposed from (a) Koch triadic fractal island, (b) Random Koch triadic fractal island, and (c) Random Koch quadric fractal island. Zones decomposed from Koch quadric fractal island are shown in Figs. 3a and 4a–f.

$(M \circ (n + 1)B))$ from nth opened version (i.e., $(M \circ nB)$). The denominator denotes the total area of ith segmented zone isolated from fractal M. The zone-wise morphologic complexity measures are computed, using zone-wise probability distribution values, based on Eq. (5):

$$H(M_i/B) = -\sum_{n=0}^{N} p_n(M_i)\log_2 p_n(M_i) \tag{5}$$

These complexity measures are further normalized by dividing with number of opening cycles, required to decay corresponding segmented zone, obtained by subtracting successive threshold opening cycle numbers, $(K_i - K_{i-1})$, according to Eq. (6):

$$\text{Norm}H(M_i/B) = \frac{H(M_i/B)}{(K_i - K_{i-1})} \tag{6}$$

These normalized complexity measures (Eq. (6)) for the six decomposed zones (Fig. 4a–f) of fractal object include 0.35, 0.31, 0.49, 0, 0.38, and 0 (Table 1). It is obvious that both zones 4 and 6 possess normalized complexity measures of zeros further supporting inference that the higher the regularity, the lesser is the complexity measure. It is interesting to note that for this quadric fractal the sum of these normalized complexity measures ($\sum_{i=1}^{I} \text{Norm}H(M_i/B)$) approximately yields the analytically derived fractal dimension of Koch Quadric fractal (i.e., [log 8/log 4] = 1.50).

This framework is also tested on the following fractal shapes: two iteration Koch triadic fractal, infinite iteration random Koch triadic fractal, and random Koch Quadric fractal shapes [20]. The morphologically significant zones decomposed from these fractal shapes according to the step-wise procedure explained earlier are shown in Fig. 5. The segmented zones are colour-coded and superimposed for better visualization (Fig. 5a–c). The estimated morphologic complexity measures and their normalized values for all the decomposed zones of respective fractal shapes are given in Table 1. This table also shows the fractal dimensions computed, via box counting method, for these fractal objects of both deterministic and random types. We opined from observing these results that there is no notably significant relationship between the zone-wise complexity measures and fractal dimensions computed by conventional box counting method. However, it is worth mentioning that fractal objects—whether they are generated deterministically or by introducing randomness—possess sub-zones (Figs. 4a–f, 5a–c) with varied degrees of spatial complexities. The sub-zones that possess zero complexity measures indicate spatial homogeneity, on contrary spatially heterogeneous.

6. Conclusions

This paper focuses on the application of mathematical morphology (1) to segment fractal object into morphologically significant zones, and (2) to compute zone-wise complexity measures. To achieve the first point, we adopted (i) non-linear morphologic multiscale opening transformation to generate fractal object at multiscales, (ii) half-plane closings to construct convex hulls of multiscale fractals, and (iii) to compute convexity measures by taking the ratio of areas of fractal and convex hull at different scales. From the relationship between scale and convexity measure, morphologic phases of fractal object are determined. These morphologic phases are taken as the basis to partition the fractal object. To achieve the second point, (i) the multiscale opened versions of fractal object that yield non-empty sets while intersecting with each corresponding partitioned zone area are considered, (ii) probability distribution values at respective scales for each segmented zone are computed, and (iii) set of zone-wise morphologic entropy values (i.e., complexity measures) is computed. A Koch Quadric fractal object of which analytically derived fractal dimension, (log 8/log 4) = 1.50, is partitioned into six morphologically significant zones, and normalized complexity measures for each decomposed zone are respectively obtained as 0.35, 0.31, 0.49, 0, 0.38, and 0. The sum of these normalized complexity measures yields 1.53. However, this observation is not significantly true with that of random Koch quadric and triadic fractal shapes. This approach to estimate the zone-wise complexity measures complement with already existing methods and it offers new insights to characterize spatial objects, and can be extended to spatial functions. We conclude that this framework is worth considering to understand or classify realistic fractal sets and/or fields according to sub-zones possessing varied degrees of complexities to explore links with the physical processes involved in the formation of fractal-like phenomena. An open question lies in further validating this entire framework by choosing numerous fractal objects and fractal functions for which analytically derived fractal dimensions are available.

Appendices

A.1. Basic transformations

We will explain simple morphological transformations including binary erosion, dilation, opening, and multiscale opening on the sets. As shown in Fig. A1, we define a set M on 2-dimensional Euclidean discrete space Z^2 and B is a structuring element (SE) of primitive size that is symmetric with respect to the origin, square in shape, and has the size of 3×3. The erosion of M by B is the collection of all points m such that B, when translated by m, is contained in the original set M, and is equivalent to intersection of all the translates. Thus, the erosion of M by B can be expressed as

$$M \ominus B = \{m : B_m \subseteq M\} = \bigcap_{b \in B} M_{-B} \tag{A1}$$

The dilation of M by B is defined as the set of all the points m which the translated B_m intersects M, and is equivalent to the union of all the translates, mathematically denoted as

$$M \oplus B = \{m : B_m \neq \emptyset\} = \bigcup_{b \in B} M_{-B} \tag{A2}$$

(a) A set *M* which consists of five points.

(b) Closing of *M* by the right vertical half-plane.

(c) Closing of *M* by the left vertical half-plane.

(d) Closing of *M* by the lower horizontal half-plane.

(e) Closing of *M* by the upper horizontal half-plane.

(f) Closing of *M* by $3\pi/4$ left half-plane.

(g) Closing of *M* by $3\pi/4$ right half-plane.

(h) Closing of *M* by $\pi/4$ right half-plane.

(i) Closing of *M* by $\pi/4$ left half-plane.

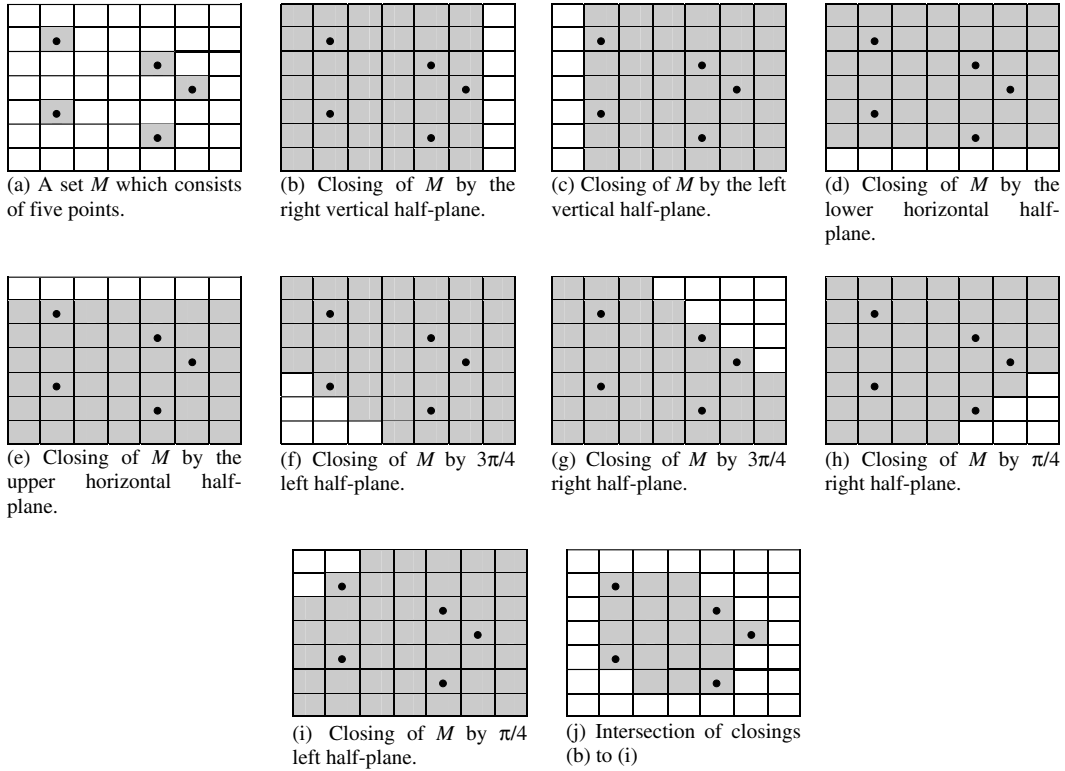(j) Intersection of closings (b) to (i)

Fig. A2. An example showing the steps resulting the convex hull of a set that consists of five pixels.

If cascade of erosion and dilation is performed, opening is obtained, and is defined as

$$M \circ B = (M \ominus B) \oplus B \tag{A3}$$

Subsequently, multiscale opening $(M \circ nB)$ can be generated by increasing the size of structuring element nB, where $n = 0, 1, 2,\ldots, N$. To produce $(M \circ nB)$ is equivalent to generating iterative opening by primitive size B for n times, as shown below:

$$M \circ nB = \{[(M \ominus B) \ominus B \ldots \ominus B] \oplus B \oplus B \ldots \oplus B\} = [(M \ominus nB) \oplus nB] \tag{A4}$$

at size $n = 0, 1, 2,\ldots, N$.

A.2. Binary convex hull

A Euclidean set *M* is convex if and only if the line segments joining any two pair of points lie entirely within the set. Consequently, a convex hull *(CH(M))* is defined as the smallest convex polygon containing all points *m* in the set *M*. It can be easily visualized by imagining an elastic band stretched open to enclose the given object. When the elastic band is released, it will assume the shape of the required convex hull. Soille [18] proposed the idea of generating convex hull of a set by intersecting all half-planes encompassing the set. For a given angle θ, there are two half-planes (denoted by π_θ^+ and π_θ^-), which correspond to this orientation, the second one being the complement of the first, i.e., $(\pi_\theta^+)^c = \pi_\theta^-$. The intersections of the half-planes for all possible orientations result in the convex hull of the set under study, mathematically denoted as

$$CH(M) = \bigcap_\theta [\phi_{\pi_\theta^+}(M) \cap \phi_{\pi_{\theta^-}}(M)] \tag{A5}$$

where $\phi_{\pi_{\theta^+}}$ represents the closings of half-planes at π_θ orientation, while $\phi_{\pi_{\theta^-}}$ symbolizes the closings with the complement of the corresponding half-plane. For better understanding, the construction of convex hull of a set *M* with simply five points is illustrated in Fig. A2. Closings of the set *M* by respective half-planes are shaded (Fig. A2b–i). In this example, eight directions of half-planes are considered, including right vertical, left vertical, lower horizontal, upper horizontal, $3\pi/4$ left, $3\pi/4$ right, $\pi/4$ right, and $\pi/4$ left. Finally, the intersection of all closings will lead to the convex hull of set *M*, as shown in Fig. A2(j). This convex hull can be taken as the smallest closed set which encloses the five points in the original set *M*.

References

[1] Feder J. Fractals. New York: Plenum Press; 1988.
[2] Korvin G. Fractal models in the earth sciences. Amsterdam: Elsevier; 1992.
[3] Robertson MC, Sammis CG, Sahimi M, Martin AJ. Fractal analysis of three-dimensional spatial distribution of earthquakes with a percolation interpretation. J Geophys Res 1995;100(B1):609–20.
[4] Douketis C, Wang Z, Haslett TL, Moskovits M. Fractal character of cold-deposited silver films determined by low-temperature scanning tunneling microscopy. Phys Rev B 1995;51(16):11022–31.
[5] Zahn W, Zösch A. The dependence of fractal dimension on measuring conditions of scanning probe microscopy. Fresenius J Analen Chem 1999;365(1-3):168–72.
[6] Halsey TC, Jensen MH, Kadanoff LP, Procaccia I, Shraiman BI. Fractal measures and their singularities: the characterization of strange sets. Phys Rev A 1986;33(2):1141–51.
[7] Flook AG. The use of dilation logic on the quantimet to achieve fractal dimension characterization of textured and structured profiles. Powder Technol 1978;21:295–8.
[8] Schroeder M. Fractals, Chaos, power laws: minutes from an infinite paradise. New York: W.H. Freeman; 1991. p. 41–5.
[9] Sagar BSD. Fractal relations of a morphological skeleton. Chaos, Solitons & Fractals 1996;7(11):1871–9.
[10] Lian TL, Radhakrishnan P, Sagar BSD. Morphological decomposition of sandstone pore-space: fractal power-laws. Chaos, Solitons & Fractals 2004;19(2):339–46.
[11] Radhakrishnan P, Teo LL, Sagar BSD. Estimation of fractal dimension through morphological decomposition. Chaos, Solitons & Fractals 2004;21(3):563–72.
[12] Sagar BSD, Chockalingam L. Fractal dimension of non-network space of a catchment basin. Geophys Res Lett 2004;31(12):L12502. doi:10.1029/2004GL019749.
[13] Chockalingam L, Sagar BSD. Morphometry of network and non-network space of basins. J Geophys Res-Solid Earth 2005;110:B08203. doi:10.1029/2005JB003641. 15 pages.
[14] Sagar BSD, Murthy MBR, Rao CB, Raj B. Morphological approach to extract ridge-valley connectivity networks from Digital Elevation Models (DEMs). Int J Remote Sens 2003;24(3):573–81.
[15] Tay LT, Sagar BSD, HT Chuah. Analysis of geophysical networks derived from multiscale digital elevation models: a morphological approach. Geosci Rem Sens Lett IEEE 2005;2(4):399–403.
[16] Sagar BSD. Universal scaling laws in surface water bodies and their zones of influence. Water Resour Res 2007;43(2):W02416–6502. doi:10.1029/2006WR005075.
[17] Mandelbrot BB. The fractal geometry of nature. New York: W.H. Freeman; 1982.
[18] Soille P. Grey scale convex hulls: definition, implementation and applications. In: Proceedings ISMM'98; 1998. p. 83–90.
[19] Lim SL, Sagar BSD. Cloud field segmentation via multiscale convexity analysis. J Geophys Res 2008; in press, doi:10.1029/2007JD009369.
[20] Peitgen H-O, Jürgens H, Saupe D. Chaos and fractals: new frontiers of science. New York: Springer; 2004.